Article

Innovative intelligent and expert system of bridges damage identification via wavelet packet energy curvature difference method integrated with artificial intelligence algorithms

Wael A. Altabey

Department of Mechanical Engineering, Faculty of Engineering, Alexandria University, Alexandria 21544, Egypt; wael.altabey@gmail.com

Abstract: Bridges are important infrastructure for highways. Monitoring their status is of great significance to ensure safe operations. In this work, a novel integrated technique from wavelet packet energy curvature difference (WPECD) and artificial intelligence (AI) for bridge damage identification is established. Initially, the damages are simulated in the bridge decks by changing the material stiffness reduction levels of bridge elements by three levels (5%, 10%, 15%) to study the effect of damage on the bridge response. Then the WPECD maps are plotted from vibration response before and after damage to the bridge for each stiffness reduction level. Unfortunately, given the nonlinearity of damage geometry, it is not easily feasible to use WPECD maps for damage identification accurately. Therefore, the (WPECD) maps are used for training a new architecture of recurrent neural networks with long short-term memory blocks (RNN-LSTM) for bridge damage identification by predicting the wavelet functions and wavelet decomposition layer effect of each node in the bridge. The effectiveness and reliability of the proposed approach were confirmed by numerical and experimental results. The performance of the proposed technique achieved high scores of accuracy, regression, and F-score equal to 93.58%, 90.43% and 88.17% respectively indicating the applicability of the proposed method for use on other important highway infrastructure.

Keywords: structural health monitoring (SHM); artificial intelligence (AI); wavelet packet energy curvature difference (WPECD); recurrent neural network with long short-term memory blocks (RNN-LSTM)

1. Introduction

Many highway infrastructures such as bridges are built through mountains and across water. The geographical environment, geological conditions, topography, and landforms are Complex, when natural disasters such as floods and heavy rains occur, it is straightforward for the highway infrastructures to collapse and generate complete or partial failure in highway flow. Safety problems in highway infrastructure generally do not occur suddenly and have symptoms [1].

It can timely monitor the environmental input, structural status parameters, and diseases of the bridge, integrate various monitoring data, regular measurement information, and analysis results, conduct an overall evaluation of the structural safety and usage status, and evaluate the working performance of the overall bridge and its main components. In this way, we can effectively control the operating status and development trend of the bridge, detect the dangerous conditions faced by the bridge structure itself and driving as early as possible, issue early warnings in the budding stage of danger in the bridge structure, and effectively avoid the occurrence of major accidents [2,3]. In this regard, there is much research that deals with different and

effective methods for establishing applicable SHM systems [4], including using AI algorithms [5] and other techniques [6–10].

The signal of the bridge structure can be locally analyzed or in space, at any time which is one of the big advantages of the wavelet method. The wavelet analysis can discover the hidden features in bridge signals that are considered to be the characteristics of the bridge structure. So the wavelet transformation method is the common method for structural damage identification [11–13]. However, the wavelet method analysis accuracy is low in the high-frequency domain, Therefore, the WPECD-based damage identification becomes a highly impacted research point [14–16]. Ding et al. [17] utilized the WPECD theory for predicting structural damage with experimental verification. Ouyang et al. [18] used symplectic geometry WPECD theory as a damage identification method for the arch bridge. Pouyan and Hosein [19] investigated on detection and quantification of damage location and severity for steel structures using wavelet packet transform for denoising the initial signals, in combination with a peak picking technique. Barbosh and Sadhu [20] proposed a damage visualization approach by leveraging the classical signal decomposition capabilities of Wavelet Packet Transformation (WPT) and the classification abilities of the Gaussian Mixture Model (GMM). Han et al. [21] confirmed experimentally for damage identification via WPECD theory. The most recent researches on structural damage identification via WPECD theory are achieved theoretically stage research because the experimental verification is very complicated, this stems from the complexity range of damage analysis of bridge structures in real situations rather than laboratory conditions.

Recently, models based on deep learning have been utilized in the data-driven approach [22]. In many platforms, the appropriate application of the models based on deep learning has been verified when dealing with large amounts of data [23]. Deep learning algorithms are classifiers that separately extract optimal characteristics from large amounts of datasets registered by sensors and simultaneously determine the health status of the structure [24]. The detection models based on deep learning need characteristics extracted from datasets to classify and determine the health status of the structure [25]. The suitable structural damage detection is based significantly on the characteristics extracted/selected. The feature extraction of damage depends on the structural characteristics, geometric, boundary conditions, and damage types, this damage may vary over time. In addition, considering the operation and environmental effects, the function of more sensitive damage to the environmental changes is extracted [26]. Sun et al. [27] integrated between WPECD approach and neural networks for damage identification in structures and they confirmed the effectiveness of their proposed method.

A typical stiffness-reduction model relates the degradation of modulus to the fraction of life expended at a given stress amplitude, assuming that the residual stiffness decreases monotonically as the number of load cycles increases. This research is a novel integrated technique from the WPECD theory with RNN-LSTM for bridge damage identification. As we will mention later, three levels of damage index by apply the stiffness reduction of modulus E_x, and E_y by (5%, 10%, 15%) selectively in some elements of the finite element model of the bridge, and then the

WPECD maps for each level that is used for training the designed RNN-LSTM. RNN-LSTM architecture is used for predicting the wavelet functions and wavelet decomposition layer effect of each node in the bridge. The effectiveness and reliability of the proposed approach were confirmed by numerical and experimental results. The performance of the proposed technique achieved high scores of accuracy, regression, and F-score that indicates the applicability of the proposed technique for use on other important highway infrastructure. The schematic description of the bridge proposed identification system is shown in **Figure 1**.
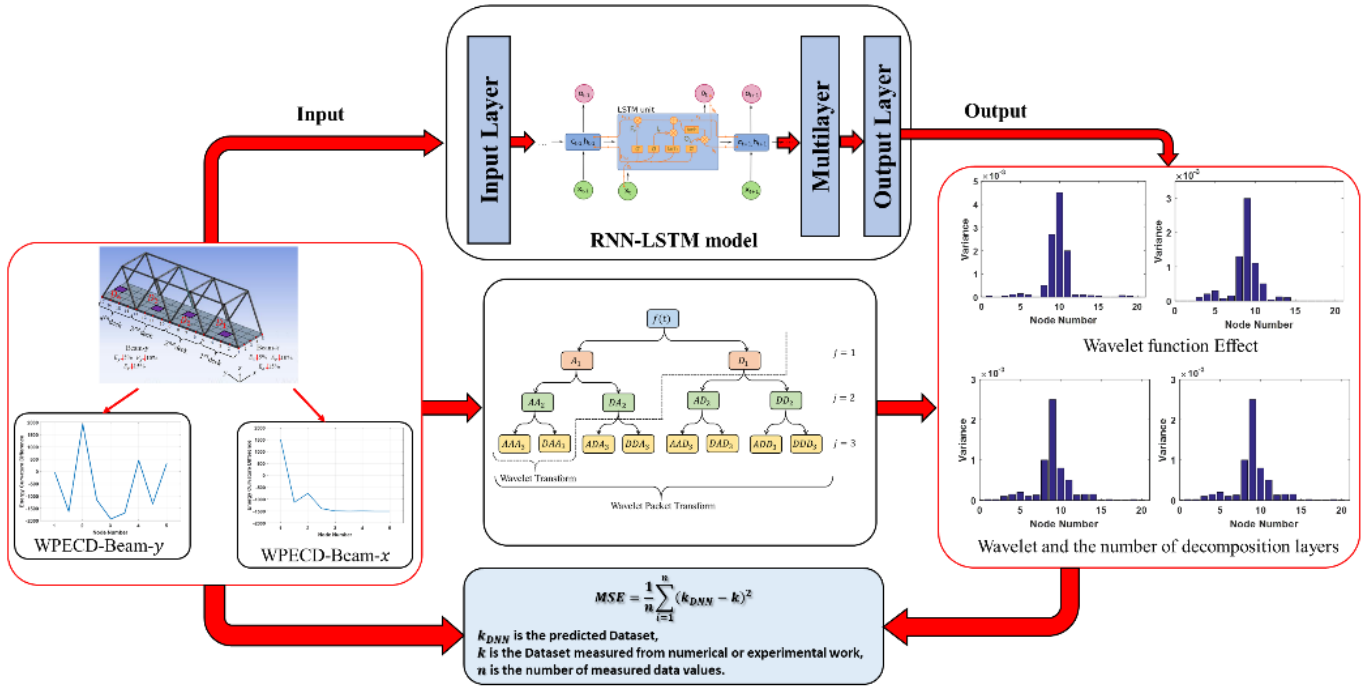

Figure 1. The schematic description of the bridge proposed monitoring system.

2. Methodology

2.1. WPECD overview

The WPECD method is a damage detection technique that utilizes the wavelet packet transform to analyze structural vibration signals, identifying potential damage locations by comparing the curvature differences in energy distribution between a healthy and damaged state across different frequency components of the signal; essentially, it highlights areas where significant changes in energy distribution occur due to damage, allowing for damage localization as we will explain later. This is a signal processing technique that decomposes a signal into multiple frequency components at different scales, providing detailed information across the frequency spectrum. The advantage of WPECD, it has High sensitivity and localization capability, is Non-invasive, and is considered a multiple-resolution method, which can have a table and the local characteristics of the signal in the time-frequency domain. Although the resolution of each wavelet decomposition layer is not similar, the sub-bands taken in each layer are stationary, and they are only decomposed in the part that has low frequency. So, for the resolution band that has high frequency, it also has the

flaws of a bad, so it only applies to certain features of waves. In each layer, sub-bands are divided into two parts and then transferred to the after layer to decompose both frequencies (low, and high). Another limitation of WPECD is the complexity intensive, especially for large datasets, the parameter selection can impact the accuracy of damage detection, and the curvature calculation sensitivity by the signal noise.

Each layer of subbands covers the frequency occupied by the original signal, but the resolution of each layer is different, as shown in **Figure 2**. The efficiency of WPECD in-signal analysis is high and it can be utilized as a multi-resolution. The parts that have high frequency and unsatisfactory analysis will be further decomposed, it can be analyzed according to the information of the analysis signal features, to modify the resolution of high-frequency, it can be selected the corresponding frequency band to identify the signal spectrum.

Usually, the WPECD function is presented by $\psi_{j,k}^i$, where i, j, k are the factors of the wavelet such as scale, translation, and modulation factors respectively, the function is evaluated as [28]:

$$\psi_{j,k}^i(t) = 2^{j/2}\psi^i(2^j t - k), (i = 1,2,\cdots) \tag{1}$$

The wavelet function repetition relationship ψ^i is:

$$\psi^{2i}(t) = \sqrt{2}\sum_{-\infty}^{\infty} h(k)\,\psi^i(2t - k) \tag{2}$$

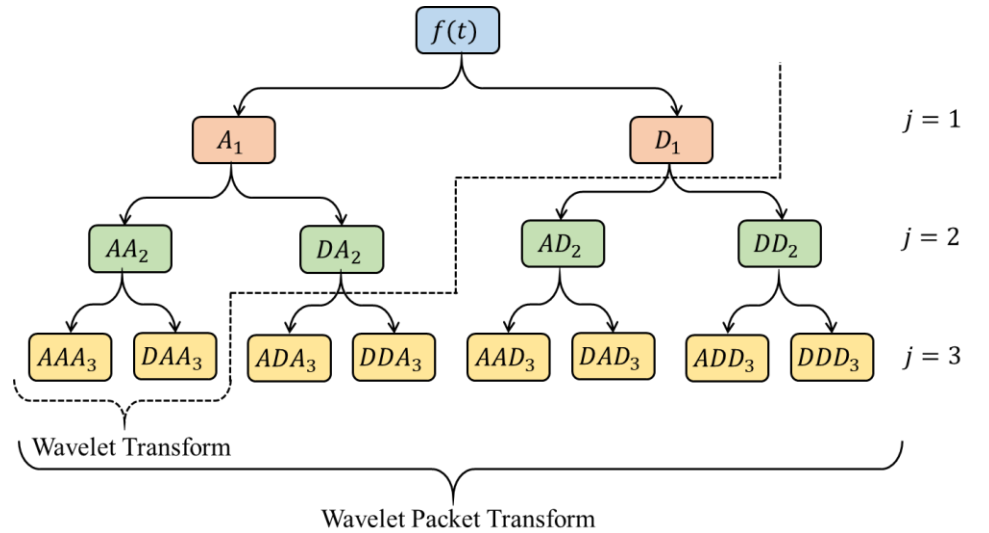$$\psi^{2i+1}(t) = \sqrt{2}\sum_{-\infty}^{\infty} g(k)\,\psi^i(2t - k) \tag{3}$$

Figure 2. Schematic of wavelet packet transform.

At Equations (2) and (3), ψ is the mother function of the wavelet, $h(k), g(k)$ are the scale functions and are associated with the mirror filter parameters, it is a small integral at any signal by wavelet mother function. j^{th} is called the repeated relationship order, and $j + 1^{th}$ is the WPECD decomposition in horizontal order:

$$f_j^i(t) = f_{j+1}^{2i-1}(t) + f_{j+1}^{2i}(t) \tag{4}$$

$$f_{j+1}^{2i-1}(t) = Hf_j^i(t) \tag{5}$$

$$f_{j+1}^{2i}(t) = Gf_j^i(t) \tag{6}$$

where: H and G coincided with the operators of the filter of $h(k)$ and $g(k)$ respectively, evaluated:

$$H\{\cdot\} = \sum_{k=-\infty}^{\infty} h(k - 2t) \tag{7}$$

$$G\{\cdot\} = \sum_{k=-\infty}^{\infty} g(k - 2t) \tag{8}$$

After the decomposition of the wavelet packet at the j level, the beginning signal $f(t)$ is expressed as:

$$f(t) = \sum_{i=1}^{2^j} f_j^i(t) \tag{9}$$

Wavelet packet component signal $f_j^i(t)$ can be computed as a wavelet packet linear function collection:

$$f_j^i(t) = \sum_{-\infty}^{\infty} c_{j,k}^i(t)\psi_{j,k}^i(t) \tag{10}$$

The computation formula for wavelet packet coefficient (WPC) is:

$$c_{j,k}^i = \int_{-\infty}^{\infty} f(t)\,\psi_{j,k}^i(t)dt \tag{11}$$

Between them, the orthogonal state of the WPC is satisfied:

$$\psi_{j,k}^m(t)\psi_{j,k}^n(t) = 0, \, m \neq n \tag{12}$$

The decomposition of the wavelet packet is often utilized in energy detection. The energy signal of the Wavelet Packet Energy is described as:

$$E_f = \int_{-\infty}^{\infty} f^2(t)\,dt = \sum_{m=1}^{2i} \sum_{n=1}^{2^j} \int_{-\infty}^{\infty} f_j^m(t)f_j^n(t)dt \tag{13}$$

By replacing Equation (10) with Equation (13), and utilizing the orthogonal state of Equation (12), we get:

$$E_f = \sum_{i=1}^{2i} E_{f_j^i} \tag{14}$$

where wavelet packet component energy $E_{f_j^i}$ can be considered as stored in the component signal $f_j^i(t)$ energy of:

$$E_{f_j^i} = \int_{-\infty}^{\infty} f_j^i(t)^2\,dt \tag{15}$$

where E_f is the signal energy $f(t)$.

Equation (14) can be analyzed as the signal total energy and it is specified by adding the WPECD energies of corresponding components to various bands of frequency.

The energies of the components are sensitive to vary in signal characteristics and can be utilized to reveal and detect the signal features. The signal response is affected by the damage to the structure. When the frequency of certain signal components decomposed by the WPECD. It is measured via a change in the signal energy distribution with the frequency for diagnosing structural damage.

2.2. RNN-LSTM configuration

As we mentioned previously, the bridge damage will be identified by integrating the WPECD technique with RNN-LSTM for bridge damage identification by using the data extracted from WPECD for training the RNN-LSTM algorithm to identify the damage features.

RNNs deeply analyze the time series data by applying the feedback loops to the original ANN [29]. The biggest disadvantage in RNNs is known as the vanishing gradient problem, where during the backpropagation process, the error signal used to train the network exponentially decreases the further you travel backward in RNN, so sometimes use computational nodes known as LSTM to relieve this problem as shown in **Figure 3**. The data feature extraction is done from the first layers of ANN. These layers are responsible for extracting significant information from the input data.

LSTM is a special type of RNN with a gating mechanism and memory cells, which greatly improve the performance of RNNs. There are three types of gates within each LSTM cell: input gate, forget gate, and output gate, and these gates define the state of each memory cell by using sigmoid as the activation function to cause information to be transmitted selectively. The memory cell that retains the long-term state c_t is the key architecture of each LSTM cell. The internal architecture of a single LSTM cell is shown in **Figure 4**.
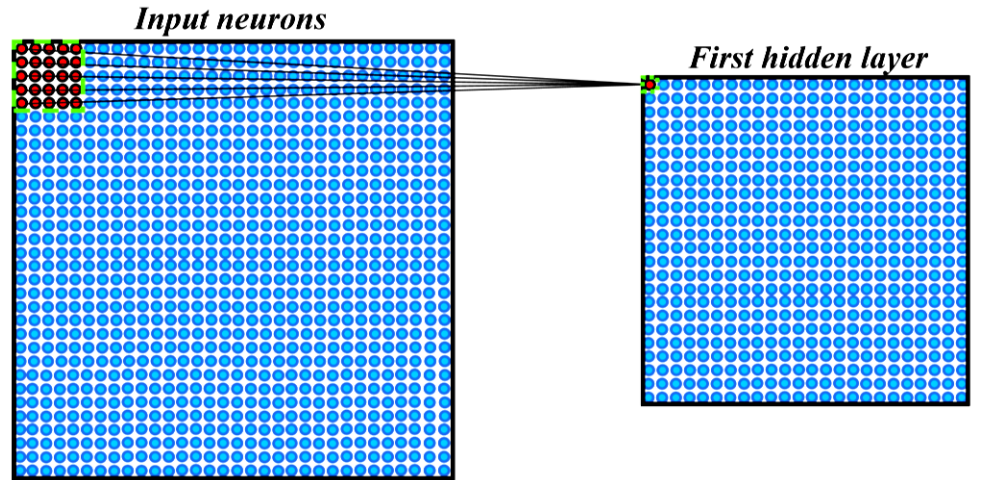

Figure 3. A 5 × 5 filter rolls around an input volume and generates an output [29].

The basic form of LSTM can be derived from:

$$o_t = \sigma(W_o \cdot [h_{t-1}, x_t] + b_o) \tag{16}$$

$$\acute{c}_t = tanh(W_c \cdot [h_{t-1}, x_t] + b_c) \tag{17}$$

$$c_t = f_t \odot c_{t-1} + i_t \odot \acute{c}_t \tag{18}$$

$$h_t = o_t \odot \tanh(c_t) \tag{19}$$

where W_f, W_i, W_c, and W_o define the weight matrices of LSTM; b_f, b_i, b_c, and b_o represent the bias vector of LSTM; f_t, i_t, and o_t her forget gate, input gate, and output gate vectors at timet; c_{t-1} and $\acute{c}_t$ mean, respectively, the previous cell condition and a

new candidate value. $\sigma(z)$ and $tanh(z)$ are used as the activation functions, as indicated below:

$$\sigma(z) = \frac{1}{1+e^{-z}} \tag{20}$$

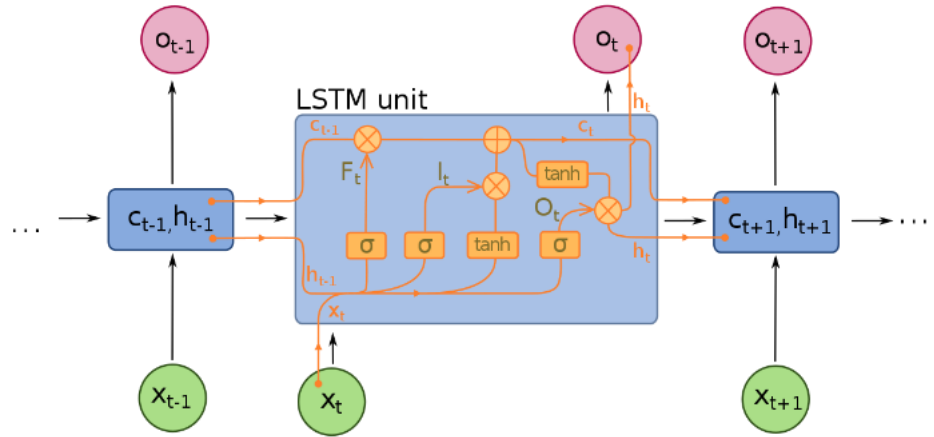$$tanh(z) = \frac{e^z - e^{-z}}{e^z + e^{-z}} \tag{21}$$

Figure 4. A single block diagram in an RNN-LSTM [30].

3. Case study

3.1. The experimental work

To evaluate the effectiveness of the WPECD Technique, an experimental work on a truss bridge was established. The sensors were installed on each bridge deck and excited using a random load on the decks as presented in **Figure 5**. As shown in the Figure, the bridge's geometric specifications are 4 m long, and 1 m high, and the bridge's structural specifications are $E = 210$ GPa elastic modulus, $G = 10.64$ GPa Shear modulus, $v = 0.3$ Poisson coefficient, and 7860 kg/m³ density. The sensor type used in this research is a wireless intelligent vibration sensor, which is one of the Lightweight Wireless sensors, as shown in **Figure 6**, the sensor performance indicators are presented in **Table 1**. **Figure 7** presents the excitation load applied to the bridge model is random excitation $(-3000 \sim 3000 \text{ kN} \pm 20 \text{ N})$ in the *x-axis* direction and simultaneously, the vibrations of specific decks were measured. The Vibration tests were conducted to bridge before and after damage for three damaged cases, where noises and measurement errors were considered to be present. The damage was simulated as changing the material stiffness reduction levels (5%, 10%, 15%) on the bridge deck element. The vibrational signals were extracted from sensors for each of the examined decks.
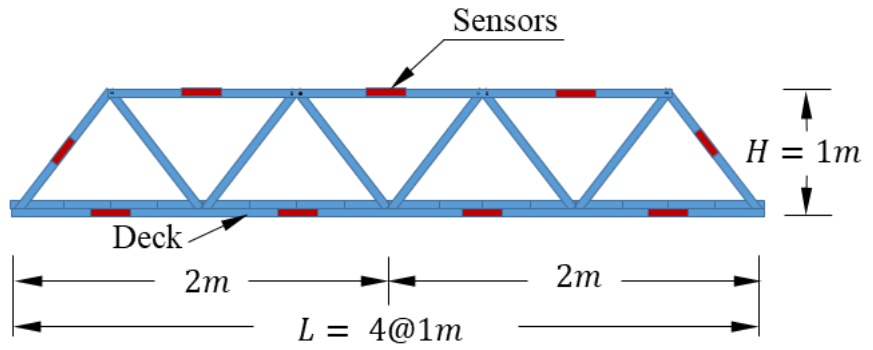
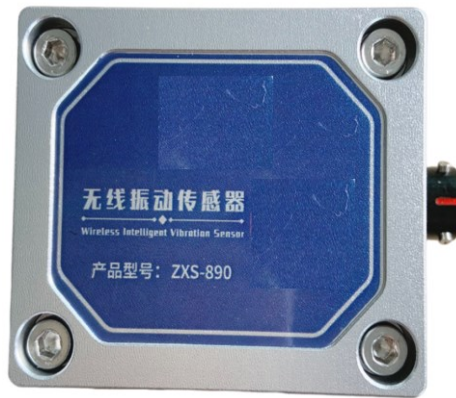**Figure 5.** Sensors install configuration on the bridge.

Figure 6. Wireless intelligent vibration sensor.

Table 1. Sensor performance indicators.

| Gear	Acceleration	Small Speed	Medium Speed	High Speed
Sensitivity V.s/m:	0.3	23	2.4	0.8
Acceleration (m/s^2) maximum range:	20	-	-	-
Speed (m/s):	-	0.125	0.3	0.6
Displacement (mm):	20	200	500	-
Passband Hz, +1/−3dB:	$0.25 \sim 80$	$1 \sim 100$	$0.25 \sim 100$	$0.17 \sim 100$
Output load resistance (kΩ):	1000	1000	1000	1000
Acceleration (m/s^2) resolution:	5×10^{-6}	-	-	-
Speed (m/s) resolution:	-	4×10^{-8}	4×10^{-7}	1.6×10^{-6}
Displacement (mm) resolution:	-	4×10^{-8}	4×10^{-7}	1.6×10^{-6}
size and weight:	$63 \times 63 \times 80$ mm, 1 kg			
Temperature environment:	−35 ℃ $\sim$ +70 ℃			
Humidity environment:	≤ 90% RH			
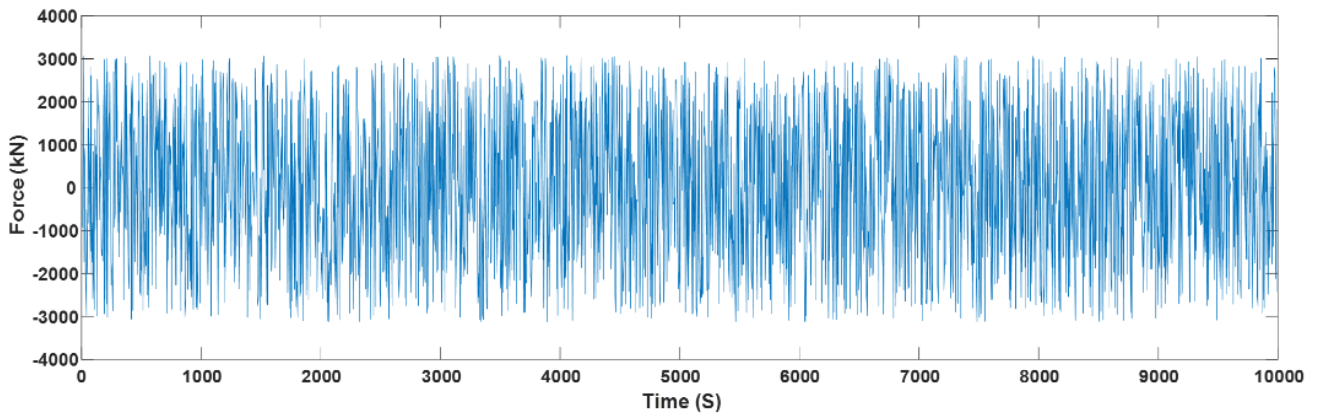
Figure 7. Random excitation.

The sensor type used in this research is a wireless intelligent vibration sensor, it's one of the Lightweight Wireless sensors.

The following steps were followed to extract the natural frequency of the experimental bridge model:

1) The model was stimulated by a random excitation (−3000 ~ 3000 kN ± 20 N) in the *x-axis* direction and simultaneously, the vibrations of specific decks were measured.

2) To calculate the natural frequency of a structure using the Fast Fourier Transform (FFT) method, you first need to acquire a time-domain vibration signal from the structure, then apply the FFT algorithm to transform the signal into the frequency domain, where the peaks in the spectrum correspond to the natural frequencies of the structure; essentially, you are identifying the frequencies at which the structure exhibits the most significant vibration amplitude.

3) Finally, the physical model natural frequency was obtained. The procedure of extracting free vibration from the experimental model of the bridge is presented in **Figure 8**. **Figure 8a** presents an example of the vibration signal measured from the 2nd deck of the bridge. As seen in the Figure the noise is very clear during the measuring. **Figure 8b** indicates the natural frequency contained in the FFT function of the signal, which is equal to (28.2 Hz).
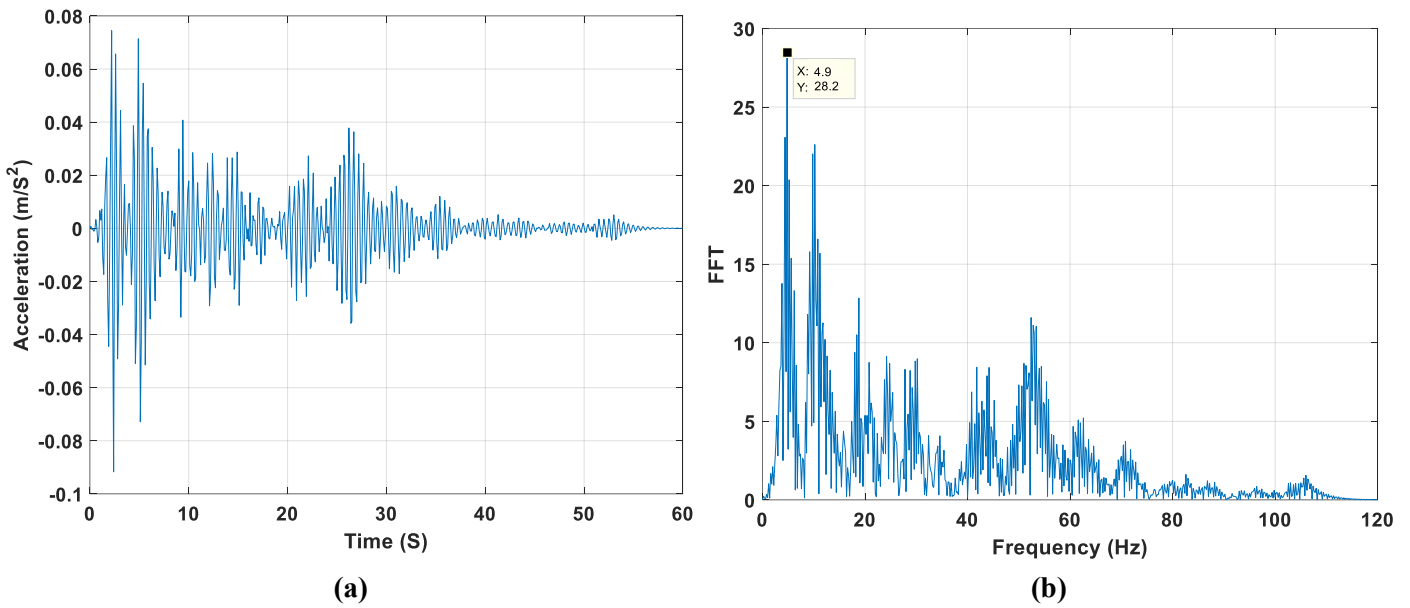
(a)   **(b)**

Figure 8. (a) The acceleration diagram associated with the 2nd deck; **(b)** the free vibration frequency of the bridge in the *x-axis* direction (experimental model).

3.2. Numerical simulation of bridge

Figure 9 presents the truss bridge numerical simulation model by ANSYS software using the same geometric and structural specifications that are used in the vibration test. The element type selection is Link1 element is used in the material model *EX* 210000 modeling structure, and the mesh size selection was done based on sensitivity analysis.
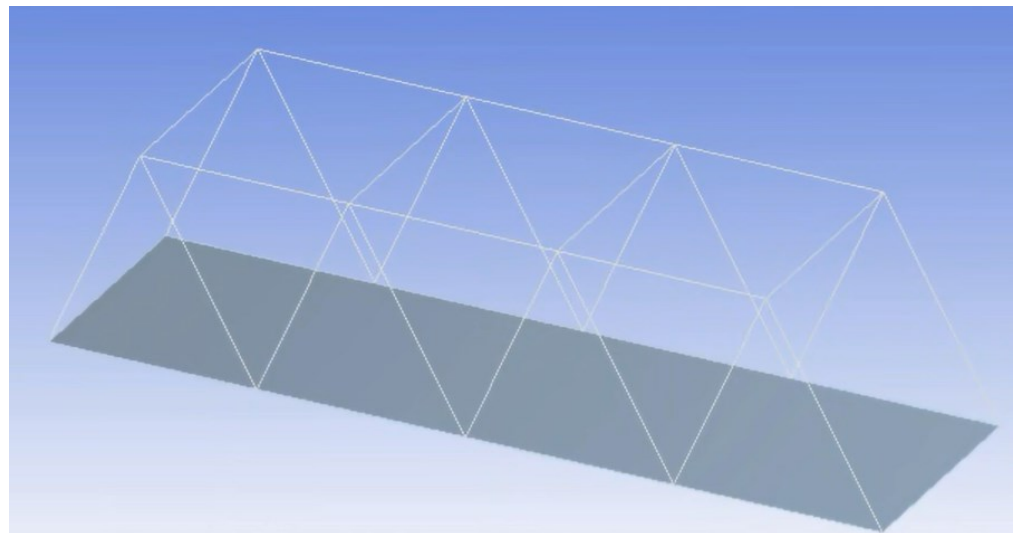

Figure 9. The numerical simulation details of the truss bridge.

3.2.1. Stress analysis

Figures 10 and **11** show bridge deformation and maximum stress respectively. As seen in the figures the maximum stress of the bridge is about 98.468 MPa, and the maximum deformation is 15.918 mm.
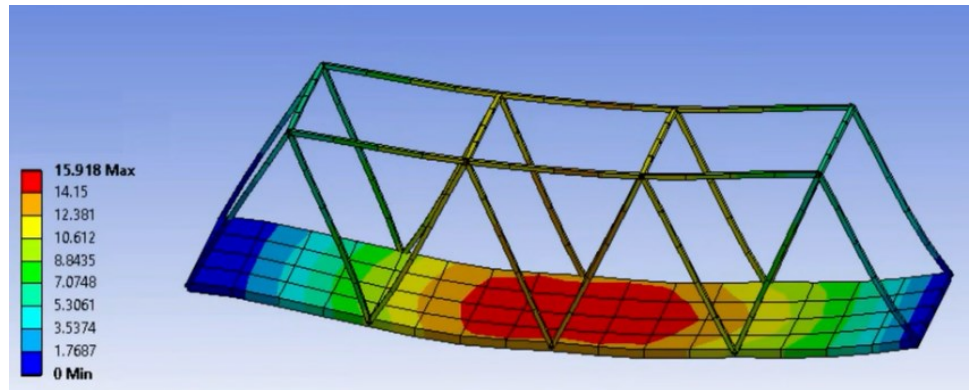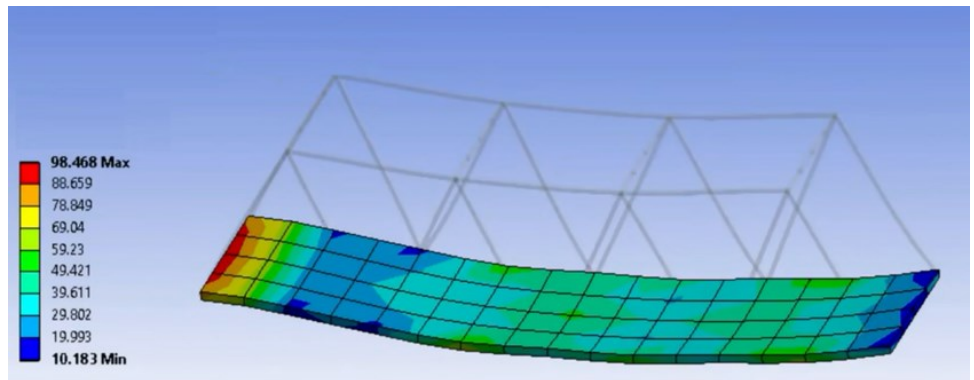
Figure 10. Displacement.

Figure 11. Von mises stress.

3.2.2. The numerical model validation

In this research, the numerical results were used to estimate the WPECD index and damage detection, thus, the numerical model validation should be done by comparing the natural frequency of the bridge in experimental and numerical models, as presented in **Figures 8** and **12**. To study the influence of the noise on the responses of the sensors, the Signal-to-noise ratio (*SNR* = 10) will be added to the numerical signal before comparing, then the FFT function was used to transfer the vibration signal from the time to frequency domain and encode it into MATLAB. Finally, the numerical model's natural frequency was obtained as shown in the Figures the error in the natural frequency is 1.45% between the experimental model (28.812 Hz) and the numerical model (28.4 Hz), which is an acceptable accuracy in validation of the numerical model results.
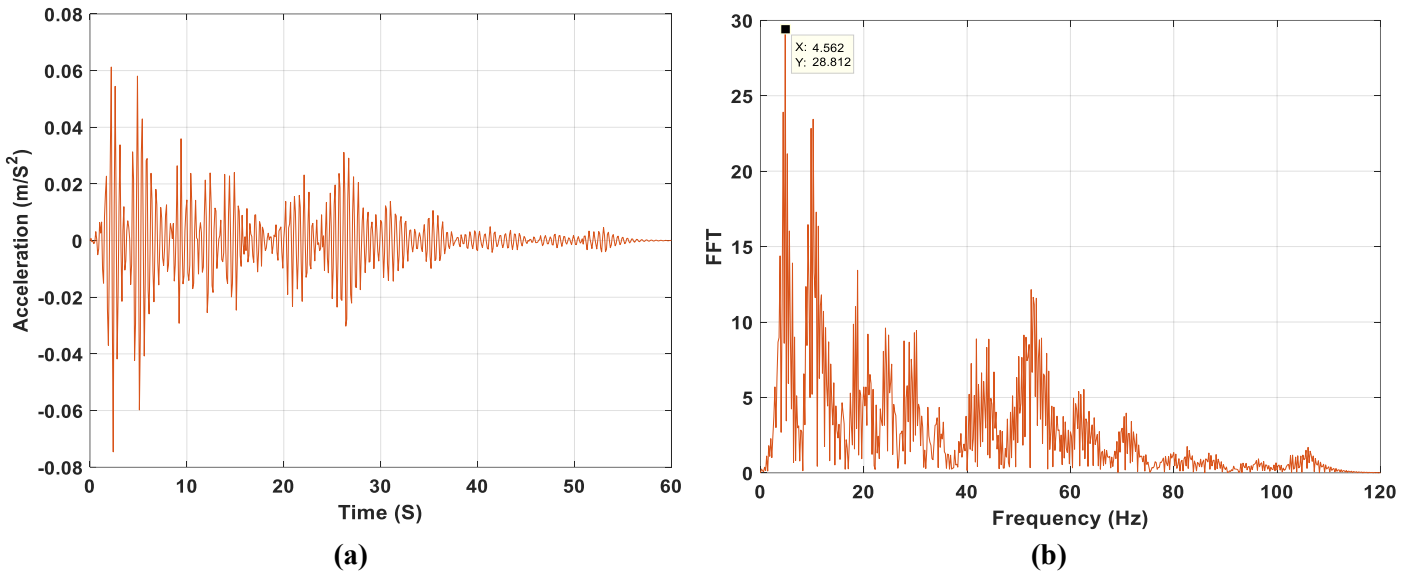
(a)

(b)

Figure 12. (a) The acceleration diagram associated with the 2nd deck; **(b)** the free vibration frequency of the bridge in the *x-axis* direction (numerical model).

3.3. The damage model

As we mentioned the bridge is loaded by random excitation, and divided into 85 and 64 for a total number of nodes and elements respectively, i.e., 4×16 elements and 5×17 nodes at x and y beam respectively as shown in **Figure 13** and **Table 2**. The damage cases (D_1, D_2, D_3, D_4) in this work as shown in **Figure 13** are considered as changes in stiffness reduction levels at the x and y beam axis by 5%, 10%, and 15% respectively and the damage location has been markered using a different color in FEM.
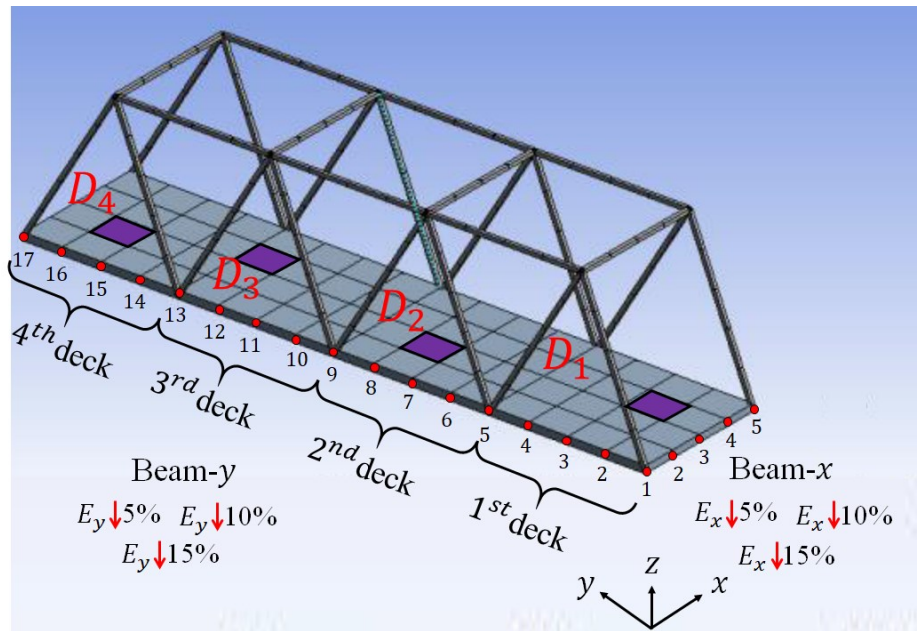

Figure 13. The damage location.

Table 2. The number of the elements and nodes at the *x* and *y* axis for each case of damage.

| Damage Case	Element number ($x - y$)	Node range at the *x-axis*	Node range at the *y-axis*
D_1	$3 - 2$	$3 - 4$	$2 - 3$
D_2	$2 - 7$	$2 - 3$	$7 - 8$
D_3	$3 - 12$	$3 - 4$	$12 - 13$
D_4	$2 - 15$	$2 - 3$	$15 - 16$

3.4. WPECD index specifications for bridge

In this work, we selected the 2nd deck of the bridge to study due to it having a high value of deformation and the sampling frequency used in this case study is 28 Hz as shown in **Figure 12**. The corresponding WPECD index curves of the 2nd deck of the bridge at *beam-x* and *beam-y* for stiffness reduction levels 5%, 10%, and 15% are plotted in **Figures 14** and **15**, respectively. As shown in the Figures, for three levels of damage equal 5%, 10%, and 15%, the value of the WPECD index for both *beam-x* and *beam-y* at the damage element has a sudden change, this indicates the extent of sensitivity of WPECD index to damages even with the low level of damage 5%. To investigate the influence of sparse measurement points on the damage identification results, a total of 5 measurement points were selected from nodes 1, 2, 3, …, and in each beam in the 2nd deck. As shown in **Figures 14** and **15**, for example, the information of damage level 5% in elements 2 and 3 is submerged, while the information of damage level 10% in element 4 was still identified, and the damage becomes more identified at the higher damage levels. It can be seen that the measurement points are too sparse and have a greater impact on the smaller degree of damage. Therefore, in the experimental work, the measurement points should be as dense as possible for the parts where damage may occur.
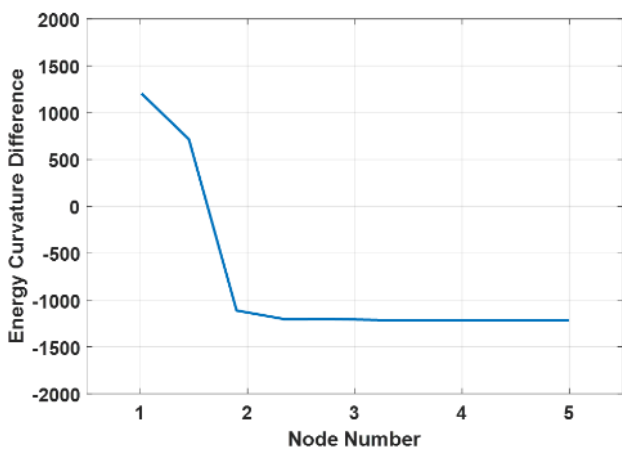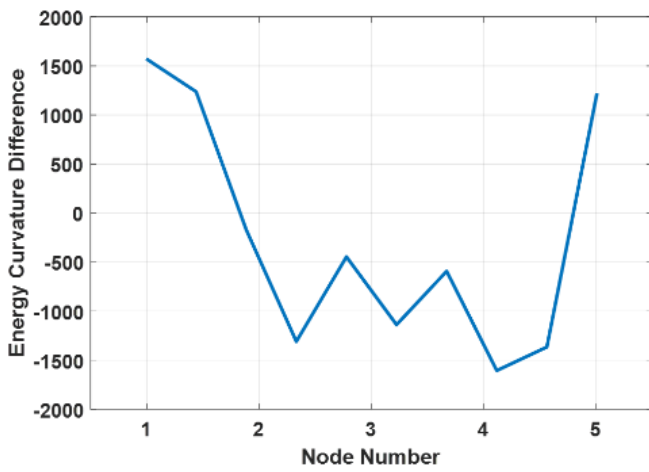

(a) 5%
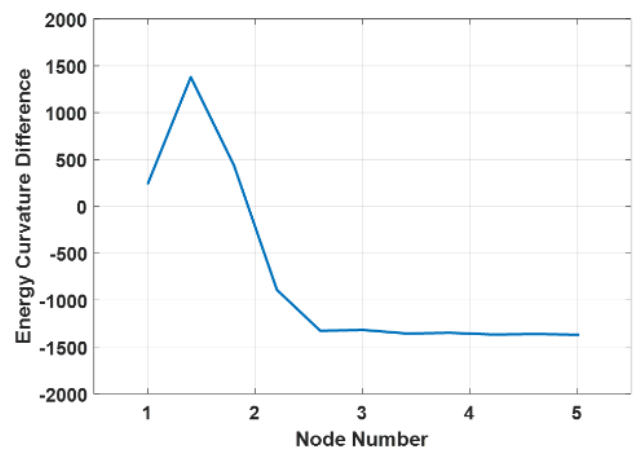
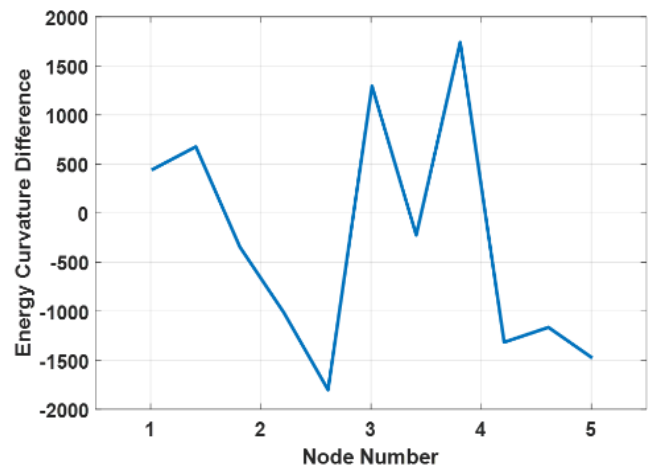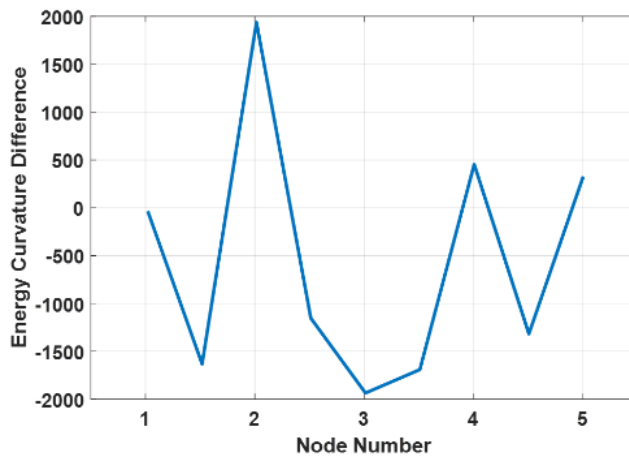

(b) 10%
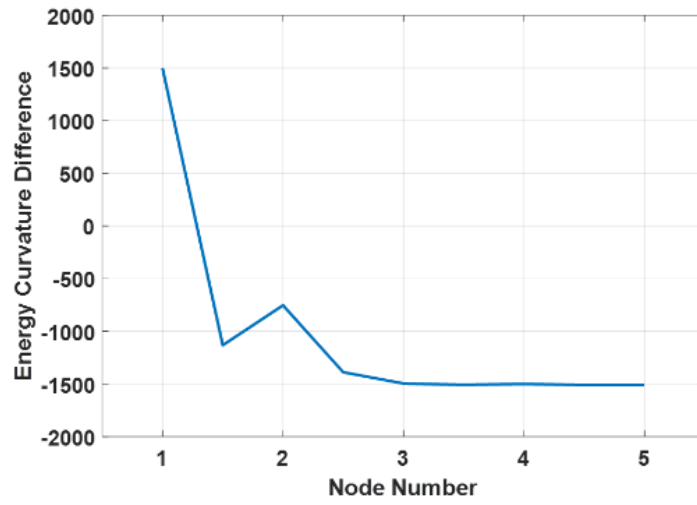
(c) 15%

Figure 14. WPECD index superposition in the *beam-x*.

(a) 5%

(b) 10%

(c) 15%

Figure 15. WPECD index superposition in the *beam-y*.

3.5. The bridge damage identification via WPECD and RNN-LSTM

As we mentioned, the main goal of using the RNN-LSTM model is predicting the wavelet functions and wavelet decomposition layer effect of each node in the bridge from the WPECD index at each damage stiffness reduction level. **Figure 16** presents the flowchart of the damage identification process using the WPECD technique and RNN-LSTM. For bridge damage identification by predicting the wavelet functions such as $Db15$ wavelet and $Coif5$ wavelet functions and wavelet decomposition layer effect of each node in the bridge are employed by training the RNN-LSTM model with WPECD maps of the 2nd deck of bridge at *beam-x* and *beam-y* for stiffness reduction levels 5%, 10%, and 15%.

The three operating conditions of each node's response are constrained by WPECD. The decomposition layers number is equal to 7, the Wavelet function is Wavelet $Db15$, and $2^7 = 128$ components and energies of WPECD coefficients, WPECD under two levels of damage.

Figure 17a,b show the $Db15$ wavelet function effect of the 2nd deck of bridge nodes components, where superposition from five components at *beam-x* and *beam-y* respectively. As shown in **Figure 17a,b**, the wavelet function $Db15$, indicates that the damage difference under the conditions of the *beam-x* is suddenly greater at node 2, and the damage position is obvious, while the damage in *beam-y* conditions, the suddenly greater change is at node 3. We can notice that the wavelet function $Db15$, has a good effect on the damage location identification.

Figure 17c,d present the results of damage identification utilizing the coif5 function effect. Through comparison between **Figure 17a,b**, and **Figure 17c,d**, we can notice the variance between the two functions of wavelet. Check the impact of many decomposition layers on the results of the wavelet recognition, and we can better see that the recognition effect occurs when the number of decomposition layers of WPECD increases.

Figure 17e,f present the results of damage identification utilized by the wavelet $Db15$ function with several decomposition layers equal to 8. Through comparison between **Figures 17a,b,e**, and **Figure 17f** we can notice that both figures have similar results of identification at almost double calculation time equal 101 s and the value of the amplitude is slightly lower.
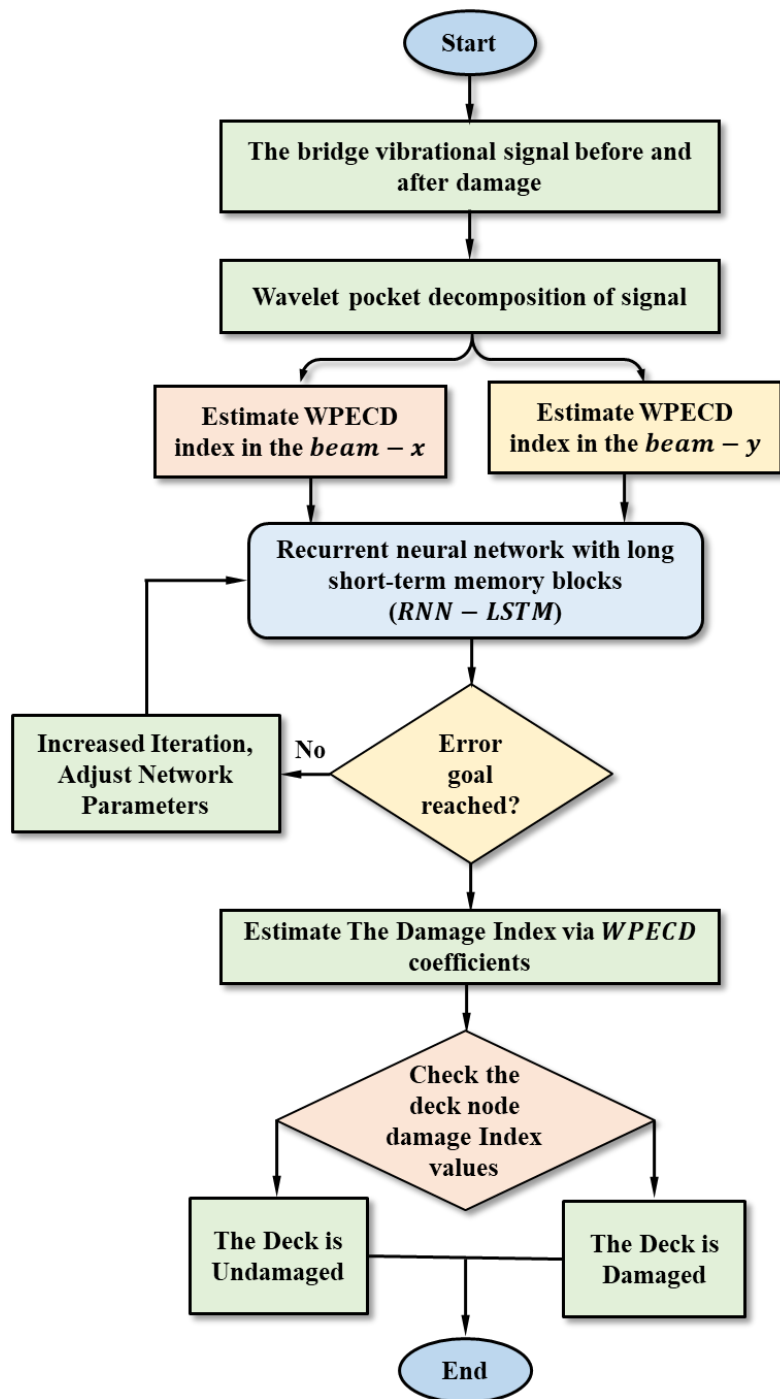
Figure 16. The Proposed approach for the damage identification process.
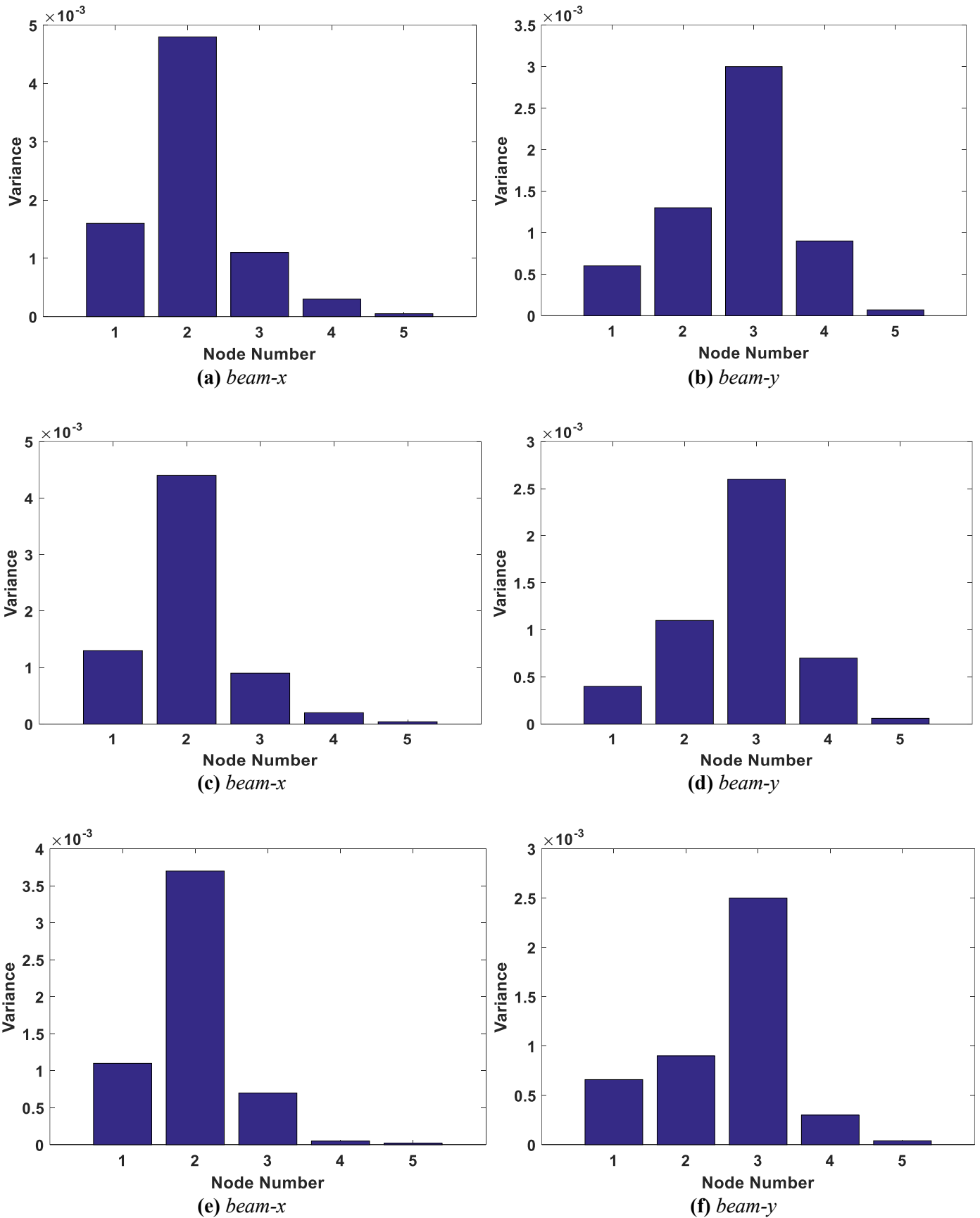
Figure 17. The damage identification results of the 2nd deck of bridge nodes components: **(a,b)** *Db*15 effect; **(c,d)** *Coif*5 effect; **(e,f)** decomposition layer effect.

3.6. The RNN-LSTM training performance

Table 3 gives the values of mean square error (MSE) (see **Figure 1**) of RNN-LSTM predicted data of damage identification of the 2nd deck of bridge at *beam-x* and *beam-y* for *Db*15, wavelet and *Coif*5 wavelet functions and wavelet decomposition layer effect. To obtain the best performances of the present RNN-LSTM. **Figure 18** presents the training and test MSE loss using supervised mode. The training key parameters are presented in **Table 4**. The steps of MATLAB code of RNN-LSTM training and evaluation are presented in Algorithm 1.

Table 3. Mean square error (MSE) values.

Wavelet functions	Direction	MSE
*Db*15	*beam-x*	0.6034
	beam-y	0.3213
*Coif*5	*beam-x*	0.1835
	beam-y	0.2552
Decomposition layer	*beam-x*	0.0935
	beam-y	0.1024

Table 4. RNN key parameters.

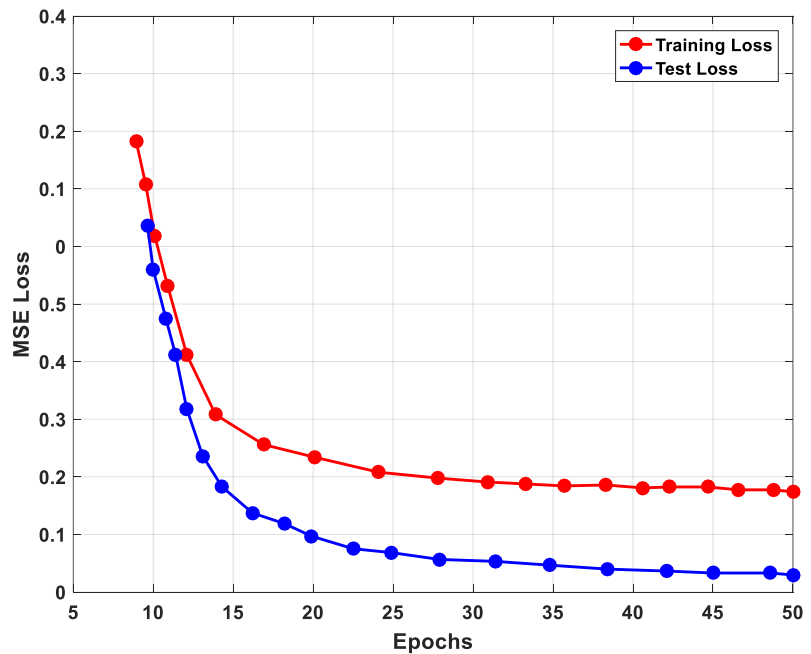| Training Time	Gauge	Training Rate	Attenuation Factor
53 sec	48	10^{-4}	10^{-6}

Figure 18. Proposed RNN-LSTM Training and testing MSE loss.

Algorithm 1 Training and evaluating of RNN

1:   **algorithm** RNN
2:   **input**: P: $p_{t,i}$ dataset, t: time $c_{t,i}$ dataset, $w_{t,i}$, S_t W: Network parameter matrix weight w_{ij} and bias b_j
3:    **output**: score of DNN trained model on test dataset to estimate bridge displacement $\alpha_{t,i}$ for various ε, EPD
4:   **let** f be the feature set 3d matrix
5:   **for** i in dataset **do**
6:    **let** f_i be the feature set matrix of sample I
7:    **for** j **in** i **do**
8:     $v_j \leftarrow$ vectorize $_{(j,\,w)}$
9:     **append** v_j to f_i
10:    **append** f_i to f
11:   f_{train}, f_{test}, l_{train}, $l_{test} \leftarrow$ split feature set and prediction into train subset and test subset
12:   M $\leftarrow$ DNN (f_{train}, l_{train})
13:   score $\leftarrow$ evaluate (I, l_{test}, M)
14:   **return** score
15: **end for**
16: **end for**

3.7. Proposed method accuracy and reliability evaluation

In this subsection, a comparison between the current method more explicitly with existing techniques using other algorithms of AI to detect the damages in bridges is presented. The performance of AI algorithms can be calibrated according to the following:

$$accuracy\ rate\ (P\%), = \frac{TPR}{TPR+FPR} \times 100 \tag{22}$$

$$regression\ rate\ (R\%) = \frac{TPR}{TPR+FNR} \times 100 \tag{23}$$

$$F\ score\ (F\%) = \frac{2TPR}{2TPR+FNR+FPR} \times 100 \tag{24}$$

where FNR is false negative rate, FPR is false positive rate, TNR is true negative rate, and TPR is true positive rate. **Tables 5** and **6** present a comparison between the current algorithm RNN-LSTM and other two algorithms used in literature to detect the damages in bridges such as convolutional neural networks (CNN) by Teng et al. [31], and Support vector machine (SVM) by Bao et al. [32].

From **Table 6**, In general for all indexes (*P*%, *R*%, *F*%, and Training Time), using CNN over the input datasets obtains a lower average accuracy than the SVM configuration, present approach RNN-LSTM achieves better results than the SVM and CNN. As a general conclusion, the proposed approach RNN-LSTM consistently outperforms the SVM, and CNN with all indexes.

Table 5. Identification performance results for RNN-LSTM and other algorithms used in literature.

Indexes	CNN	SVM	RNN-LSTM
TPR	21.34%	35.67%	48.4%
TNR	26.78%	36.36	48.34%
FPR	2.22%	2.64%	2.66%
FNR	6.25%	3.75%	2.5%

Table 6. Comparison of the test results of the RNN-LSTM and other algorithms used in literature.

Performance	CNN	SVM	RNN-LSTM
P%	90.58%	93.11%	94.79%
R%	89.66%	90.74%	91.34%
F%	86.35%	88.21%	89.16%
Training Time (sec)	112	206	53

4. Conclusion

In this research, a technique of the WPECD theory with RNN-LSTM for truss bridge damage identification was integrated. Three levels of stiffness reduction in selected bridge elements were inserted (5%, 10%, 15%), and then the WPECD maps before and after damage for each level were plotted. The wavelet functions and wavelet decomposition layer effect of each node in 2nd deck of the bridge were predicted using RNN-LSTM architecture. We found that the different wavelet functions such as $Db15$, and $Coif5$ have excellent abilities in the location of the damage identifying, the more layers of the wavelet decomposition of the damaged position, the more time consumption and comprehensive inspection of the required and extensive inspection. The effectiveness and reliability of the proposed approach were confirmed by numerical and experimental results. Considering identification effect and calculation efficiency RNN-LSTM achieved high rates of P%, R%, and F% equal to 93.58%, 90.43%, and 88.17% respectively. Results indicated the effectiveness of the approach provided, which confirms its applicability to other important highway infrastructure.

Conflict of interest: The author declares no conflict of interest.

References

1. Koh BH, Dyke SJ. Structural health monitoring for flexible bridge structures using correlation and sensitivity of modal data. Computers & Structures. 2007; 85(3-4): 117-130. doi: 10.1016/j.compstruc.2006.09.005
2. Yu Y, Ma W. A Multi-Excitation Method of Damage Detection in Plate-Like Structure Based on Wavelet Packet Energy. International Journal of Structural Stability and Dynamics. 2022; 22(08). doi: 10.1142/s0219455422500912
3. Kim H, Melhem H. Damage detection of structures by wavelet analysis. Engineering Structures. 2004; 26(3): 347-362. doi: 10.1016/j.engstruct.2003.10.008
4. Moravvej M, El-Badry M. Reference-Free Vibration-Based Damage Identification Techniques for Bridge Structural Health Monitoring—A Critical Review and Perspective. Sensors. 2024; 24(3): 876. doi: 10.3390/s24030876
5. Li ZD, He WY, Ren WX, et al. Damage detection of bridges subjected to moving load based on domain-adversarial neural network considering measurement and model error. Engineering Structures. 2023; 293: 116601. doi: 10.1016/j.engstruct.2023.116601
6. Zhou L, Hong We, Altabey WA. Bridges Damage Assessment Techniques Improvement Through Machine Learning Algorithm. In: Proceedings of the 5th International Conference on Advances in Civil and Ecological Engineering Research; 2024. doi: 10.1007/978-981-99-5716-3_6
7. Guo D, Hong W, Altabey WA. Monitoring of Bridges Damage Based on the System Transfer Function Maps from Sensors Datasets. In: Proceedings of the 5th International Conference on Advances in Civil and Ecological Engineering Research; 2024. doi: 10.1007/978-981-99-5716-3_5

8. Yang YB, Chen L, Wang ZL, et al. Cancellation of resonance for elastically supported beams subjected to successive moving loads: Optimal design condition for bridges. Engineering Structures. 2024; 307: 117950. doi: 10.1016/j.engstruct.2024.117950

9. Zhu XQ, Law SS. Wavelet-based crack identification of bridge beam from operational deflection time history. International Journal of Solids and Structures. 2006; 43(7-8): 2299-2317. doi: 10.1016/j.ijsolstr.2005.07.024

10. Wang ZL, Tan ZX, Chen L, et al. Internal and External Cancellation Conditions for Free Vibration of Damped Simple Beams Traversed by Successive Moving Loads. International Journal of Structural Stability and Dynamics. 2023; 23(16n18). doi: 10.1142/s0219455423400072

11. Oliver GA, Pereira JLJ, Francisco MB, et al. Wavelet transform-based damage identification in laminated composite beams based on modal and strain data. Mechanics of Advanced Materials and Structures. 2023; 31(19): 4575-4585. doi: 10.1080/15376494.2023.2202016

12. Hong W, Li H, Xu Y, et al. Damage identification in bridges based on WPECD transform. In: Proceedings of the 22nd International Scientific Conference Engineering for Rural Development Proceedings; 2023. doi: 10.22616/erdev.2023.22.tf211

13. Silik A, Wang X, Mei C, et al. Development of Features for Early Detection of Defects and Assessment of Bridge Decks. Structural Durability & Health Monitoring. 2023; 17(4): 257-281. doi: 10.32604/sdhm.2023.023617

14. Xiao M, Zhang W, Zhao Y, et al. Fault diagnosis of gearbox based on wavelet packet transform and CLSPSO-BP. Multimedia Tools and Applications. 2022; 81(8): 11519-11535. doi: 10.1007/s11042-022-12465-3

15. Razavi M, Hadidi A. Structural damage identification through sensitivity-based finite element model updating and wavelet packet transform component energy. Structures. 2021; 33: 4857-4870. doi: 10.1016/j.istruc.2021.07.030

16. Chen L, Lu X, Deng D, et al. Optimized Wavelet and Wavelet Packet Transform Techniques for Assessing Crack Behavior in Curved Segments of Arched Beam Bridges Spanning Rivers. Water. 2023; 15(22): 3977. doi: 10.3390/w15223977

17. Ding Y, Li A, Miao C. Invistigation on structural damage method based on wavelet packet energy spectrum. Journal of Engneering Mechanics. 2006.

18. Ouyang T, Cheng L, Li Y, et al. A novel damage identification method for arch bridge using symplectic geometry wavelet packet energy. Structures. 2024; 61: 105959. doi: 10.1016/j.istruc.2024.105959

19. Pouyan F, Hosein N. Damage Severity Quantification Using Wavelet Packet Transform and Peak Picking Method. Practice Periodical on Structural Design and Construction. 2021; 27(1). doi: 10.1061/(ASCE)SC.1943-5576.0000639

20. Barbosh M, Sadhu A. Wavelet packet transformation-based improved acoustic emission method for structural damage identification. Smart Materials and Structures. 2024; 34(1): 015036. doi: 10.1088/1361-665x/ad9dc8

21. Han J, Ren W, Sun Z. Experimental study on structural damage identification based on wavelet packet analysis. Journal of Vibration and Shock. 2006.

22. Altabey WA, Noori M, Wu Z, et al. Enhancement of Structural Health Monitoring Framework on Beams based on k-Nearest Neighbor Algorithm. In: Proceedings of the 14th International Workshop on Structural Health Monitoring (IWSHM 2023): Statistical Methods and Machine Learning; 2023.

23. Moghadam KY, Noori M, Silik A, et al. Damage Detection in Structures by Using Imbalanced Classification Algorithms. Mathematics. 2024; 12(3): 432. doi: 10.3390/math12030432

24. Altabey WA, Kouritem SA, Al-Moghazy MA. A new diagnostic system for damage monitoring of BFRP plates. e-Prime - Advances in Electrical Engineering, Electronics and Energy. 2023; 5: 100258. doi: 10.1016/j.prime.2023.100258

25. Altabey WA, Kouritem SA, Al-Moghazy MA. Apply frequency response function schemes for damage detection in composite nanoscale-pipes under transient conditions. Nano-Structures & Nano-Objects. 2024; 39: 101259. doi: 10.1016/j.nanoso.2024.101259

26. Altabey WA. A comprehensive study of a long-term creep thermo-mechanical fatigue behavior monitoring of BFRP composite pipeline using electrical capacitance sensors and deep learning algorithm. International Journal of Fatigue. 2024; 184: 108277. doi: 10.1016/j.ijfatigue.2024.108277

27. Sun Z, Chang CC. structural damage assessment based on wavelet packet transform. Journal of Structural Engineering. 2002; 128(10): 1354-1361. doi: 10.1061/(ASCE)0733-9445(2002)128:10(1354)

28. Karami V, Chenaghlou MR, Gharabaghi ARM. A combination of wavelet packet energy curvature difference and Richardson extrapolation for structural damage detection. Applied Ocean Research. 2020; 101: 102224. doi: 10.1016/j.apor.2020.102224

29. Hutter F, Hoos HH, Leyton-Brown K. Sequential model-based optimization for general algorithm configuration. In: Learning and Intelligent Optimization. Springer: Berlin/Heidelberg, Germany; 2011.

30. Cha Y, Choi W, Büyüköztürk O. Deep Learning-Based Crack Damage Detection Using Convolutional Neural Networks. Computer-Aided Civil and Infrastructure Engineering. 2017; 32(5): 361-378. doi: 10.1111/mice.12263

31. Teng S, Chen X, Chen G, et al. Structural damage detection based on convolutional neural networks and population of bridges. Measurement. 2022; 202: 111747. doi: 10.1016/j.measurement.2022.111747

32. Bao Y, Song C, Wang W, et al. Damage Detection of Bridge Structure Based on SVM. Mathematical Problems in Engineering. 2013; 2013: 1-7. doi: 10.1155/2013/490372